Quantum Many-Body Simulation using Cavity Coupled Monolayer Excitons

Jian-Hua Jiang,[1,*] HaiXiao Wang,[1] Alan Zhan,[2] YaDong Xu,[1] HuanYang Chen,[1] and Arka Majumdar[2,3,†]

[1] *School of Physical Science and Technology, Soochow University, 1 Shizi Street, Suzhou 215006, China*
[2] *Department of Physics, University of Washington, Seattle, Washington 98195, USA*
[3] *Department of Electrical Engineering, University of Washington, Seattle, Washington 98195, USA*

(Dated: March 9, 2016)

We propose an architecture for quantum simulation of strongly interacting bosons using monolayer excitons in MoS_2 quantum dots. The strongly coupled monolayer exciton and cavity photon form polaritons between which the interaction reaches $1 \sim 10$ meV—more than one order of magnitude higher than the state-of-art value. We discuss Mott transition in a chain of coupled cavities driven by photon blockade and polariton blockade. The cavity system can mimic optical lattices and superlattices in cold atomic systems. Our proposal suggests a promising route toward photonic simulation of strongly correlated quantum states.

PACS numbers: 42.50.Pq,42.50.Ar,42.50.Dv,78.67.Hc

arXiv:1603.02394v1 [cond-mat.mes-hall] 8 Mar 2016

Introduction.— Solving strongly correlated quantum many-body systems exactly is a formidable task. One promising approach is to mimic such complicated systems using another simpler and easily controllable quantum system, as envisioned by Feynman[1]. To that end, the first demonstration of quantum phase transitions with ultracold atoms in an optical lattice sparked a significant amount of research on quantum simulation with atomic systems[2, 3]. Interacting photons also provide an unique platform to study strongly correlated quantum many-body phenomena[4, 5]. The main idea of this approach is to obtain a correlated "quantum fluid of light"[6] by building a coupled network of nonlinear electromagnetic cavities[4, 5, 7]. Advantages of photonic quantum many-body simulation include much higher temperature/energy-scale, nondestructive and direct measurements of quasiparticle correlations via single- or two-photon interference of the luminescence, as well as abundant optical and material methods for coherent control[6].

Polariton, a quantum superposition of photon and exciton, emerges in hybrid systems of photonic microcavity and semiconductor excitons when exciton and photon interact strongly with each other[7, 8]. The half-light, half-matter nature of polaritons leads to many unusual properties: high-temperature Bose-Einstein condensation (BEC)[8–11], and enhanced optical nonlinearity for applications in all-optical diodes[12] and transistors[13]. However, optical nonlinearity in those systems are promoted by high polariton densities (i.e., one polariton interacts with many others). Achieving optical nonlinearity at the single photon level requires reducing both the extent of the active material and the area of the optical cavity mode[14]. Photon blockade has been observed when a very small quantum dot (QD) is coupled with a cavity photon[15–18]. In those systems Pauli blockade forbids double occupancy of excitons, and the interaction between polaritons is given by $U_{pl} = (2-\sqrt{2})\hbar\Omega$ with $\hbar\Omega$ being the exciton-photon coupling[15–17]. As the area of the QD is much smaller than the cavity modal area, $\hbar\Omega$ is very small, resulting in polariton interaction less than 30 μeV[18]. Strong polariton interaction, a crucial prerequisite for quantum simulation of strongly interacting bosons, has yet to be achieved.

In this work we propose a scheme exploiting the strong light-matter and exciton-exciton interactions in MoS_2 QDs to realize polariton interaction as strong as 1∼10 meV. The H1 cavity in a 2D photonic crystal is capable of enhancing both the light-matter and the exciton-exciton interaction when coupled with a MoS_2 QD due to its small mode area and mode volume[19]. We find that compared with commonly used quantum confined structures, MoS_2 monolayer is more advantageous for strongly interacting quantum photonic systems. The strongest interaction between polaritons at exciton-photon resonance is close to 1 meV, considerably higher than other materials used in the community. In addition, the atomically thin MoS_2 monolayer is chemically and mechanically stable and robust[20–22]. The state-of-art fabrication technology that allows control of the position and of the lateral size of the quantum dot while maintaining the spin-valley polarization in the material[23]. Our proposal is based on recent advancements on light-matter coupling in transition metal dichalcogenide monolayer[24–29], as well as progresses in exploiting dichalcogenide monolayer for single quantum emitters[30–33].

Material and Photonic Architecture.— The proposed architecture is illustrated in Fig. 1(a). The cavity mode is a defect mode formed by a point defect in a 2D hexagonal photonic crystal slab (called as H1 cavity)[19] [see Supplementary Materials for details]. The MoS_2 QD is placed at the center of the cavity. A network of the cavity-QD hybrid structure forms an interacting polariton lattice system, which is described by the following

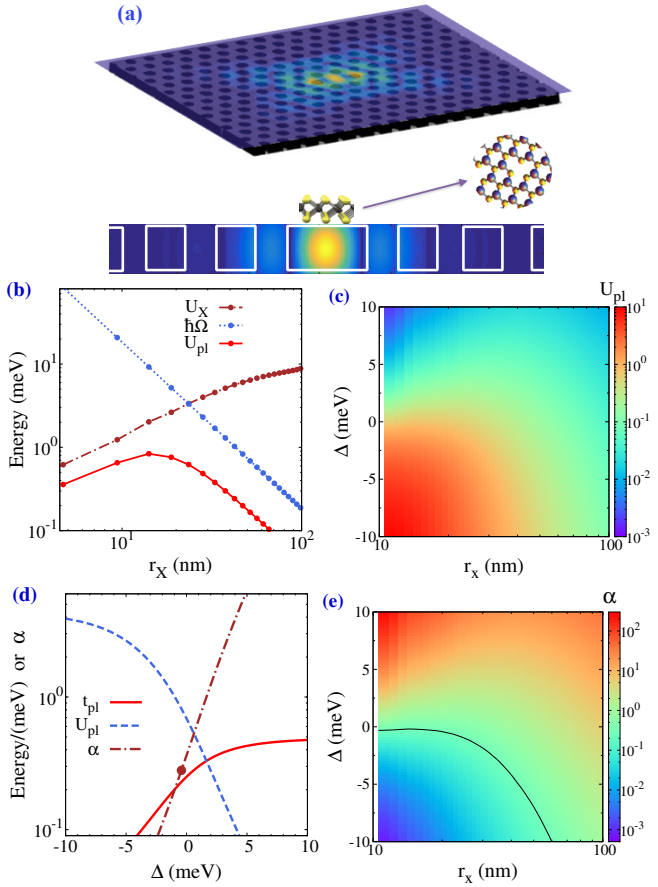

FIG. 1. (a) Cavity-QD hybrid system for strongly interacting polaritons. Upper pannel: The H1 cavity is realized using a very thin 2D photonic crystal slab. A MoS_2 QD is placed at the center of the cavity. Inplane electric field distribution at the top surface of the slab is illustrated by color. Lower pannel: Inplane electric field distribution in the x-z plane (field outside the membrane is not plotted). The position of the MoS_2 QD is illustrated using the atomic structure of MoS_2. (b) Exciton-exciton interaction U_X, exciton-photon interaction $\hbar\Omega$, and polariton-polariton interaction U_{pl} as functions of the QD radius r_X for MoS_2. (c) Polariton-polariton interaction U_{pl} vs. r_X and exciton-photon detuning Δ. (d) Polariton hopping energy t_{pl}, polariton-polariton interaction U_{pl}, and the coefficient $\alpha \equiv t_{pl}/U_{pl}$ as functions of detuning Δ for MoS_2 circular QD with radius $r_X = 20$ nm and $t = 0.5$ meV. (e) α and phase diagram for strongly interacting 1D polariton system for various MoS_2 QD radius r_X and exciton-photon detuning Δ with hopping energy $t = 0.5$ meV.

Hamiltonian[6]

$$\mathcal{H} = \sum_i \big[\hbar\omega_c c_i^\dagger c_i + \hbar\omega_X b_i^\dagger b_i + \hbar\Omega(c_i b_i^\dagger + b_i c_i^\dagger) + \frac{1}{2}U_X \mathcal{N}_i(\mathcal{N}_i - 1) + \big] - t\sum_{\langle i,j\rangle} c_i^\dagger c_j, \quad (1)$$

Here ω_c is the frequency of the localized photon mode in each cavity, $c_i^\dagger$ ($b_i^\dagger$) creates a photon (exciton) in the i^{th} cavity-QD element ($\mathcal{N}_i = b_i^\dagger b_i$ is the exciton number operator), and $\hbar\omega_X = 1.87$ eV is the exciton energy in MoS_2. We have assumed that ω_c is identical for each cavity and ω_X is the same for each MoS_2 QD. We shall discuss later the situations when they vary for different cavities and QDs (including designated modulation and fluctuations). The collective exciton-photon coupling is written as[8, 11]

$$\hbar\Omega = \frac{d_{cv}|\phi(0)|\sqrt{\hbar\omega_c}}{\sqrt{2\epsilon_0 L_c}}, \quad (2)$$

where $d_{cv} = 4.0 \times 10^{-29}$ C·m is the interband dipole matrix element[11, 26] and $|\phi(0)| = \sqrt{2/(\pi a_B^2)}$ is the exciton wave amplitude at zero electron-hole distance ($a_B = 1$ nm is the exciton Bohr radius in MoS_2[34]). The exciton-photon coupling depends on the quantity

$$L_c \equiv \frac{\int_c d\vec{r}\epsilon(\vec{r})|\vec{E}(\vec{r})|^2}{\int_c dxdy|\vec{E}(x,y,z_0)|^2\Theta(x,y,z_0)}, \quad (3)$$

where $\epsilon(\vec{r})$ is the position-dependent (relative) dielectric function, $\vec{E}(\vec{r})$ is the electric field of the cavity mode, and z_0 is the z coordinate of the MoS_2 monolayer. The $\Theta(x, y, z_0)$ function, which takes into account of the finite overlap between the QD and the cavity optical field, is 1 in the QD region and 0 outside[8]. The integrals are carried out within each cavity. The exciton-exciton interaction is given by[35] $U_X = \frac{6E_b a_B^2}{S_X}$, where $E_b = 0.96$ eV is the exciton binding energy and $S_X = \pi r_X^2$ is the area of the circular MoS_2 QD with radius r_X. The last term in Eq. (1) describes photon hopping between nearest-neighbor cavities, where t is the hopping energy.

Our H1 cavity with slab thickness of 110 nm has modal-volume $0.45(\lambda/n)^3$ and modal-area $1.0(\lambda/n)^2$ for the fundamental mode, which is suitable for simultaneous strong light-matter interaction and strong exciton-exciton repulsion. Here $\lambda = 660$ nm is the (vacuum) wavelength of the photon in resonance with the MoS_2 exciton. The photonic crystal can be fabricated using GaP which has a refractive index $n = 3.2$. With photonic lattice constant $a = 190$ nm, the TE-like cavity mode is in resonance with the monolayer exciton.

Mott transition in strongly interacting 1D polariton lattice.— The strongly correlated polaritonic Mott insulator phases emerge only in the regime with $U_X, \hbar\Omega \gg t$. The full Hamiltonian can then be truncated into the lower polariton Hilbert space, giving rise to

$$\mathcal{H}_{pl} = -t_{pl}\sum_{<i,j>} a_i^\dagger a_j + \frac{1}{2}\sum_i U_{pl} n_i(n_i - 1), \quad (4)$$

where $t_{pl} = tp_c$ and $n_i = a_i^\dagger a_i$ with $a_i^\dagger$ being polariton creation operator. $p_c \equiv \cos^2[\frac{1}{2}\mathrm{arccot}(\frac{\Delta}{2\hbar\Omega})]$ is the photonic fraction of the lower polariton with $\Delta \equiv \hbar(\omega_X - \omega_c)$ denoting the exciton-photon detuning[6]. The polariton

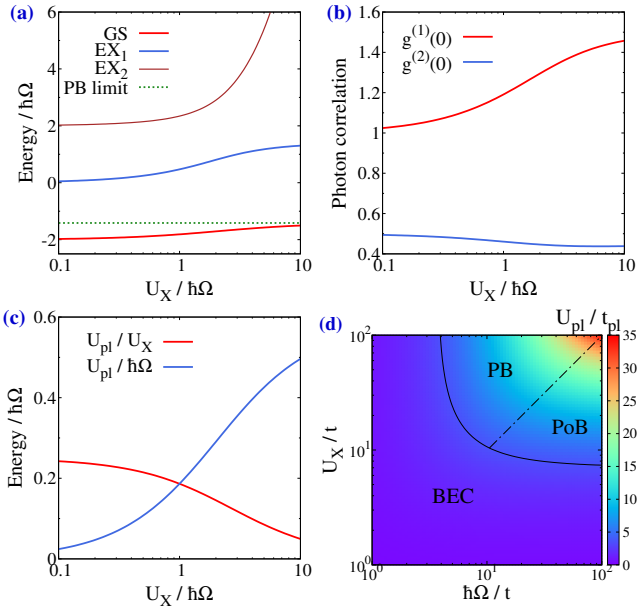

FIG. 2. Crossover from polariton blockade to photon blockade. (a) Energy levels of the ground state (GS), the first and second excited states (EX_1 and EX_2) as functions of the exciton-exciton interaction U_X. To demonstrate the crossover, we scale the interaction energy U_X with the exciton-photon coupling $\hbar\Omega$. The dotted line denote the energy $-\sqrt{2}\hbar\Omega$, i.e., the GS energy in the photon blockade (PB) limit. Energy zero is set to $\hbar\omega_c = \hbar\omega_X$. (b) Photon correlation function $g^{(1)}(0)$ and $g^{(2)}(0)$ as functions of $U_X/(\hbar\Omega)$. (c) Polariton interaction energy U_{pl} for various $U_X/(\hbar\Omega)$. (d) α and phase diagram of 1D interacting polaritons with zero detuning. The Mott insulator phase consists two regions: the photon blockade (PB) region and the polariton blockade (PoB) region. The phase boundary between BEC and Mott insulator is labeled by the solid curve, while the crossover between PB and PoB regions is labeled by the chained curve.

interaction U_{pl} is calculated as $U_{pl} \equiv E_{GS}(2) - E^0_{GS}(2)$ where $E_{GS}(2)$ [$E^0_{GS}(2)$] is the ground state energy with [without] interaction. For 1D systems considered in this work, the quantum phase transition from the BEC phase to the Mott insulator phase takes place at $\alpha = \alpha_c$ ($\alpha \equiv t_{pl}/U_{pl}$) with $\alpha_c = 0.28$ for filling factor $\nu = 1$[38] (i.e., one polariton per cavity).

The polariton interaction U_{pl} has nonmonotonic dependence on the QD radius [Fig. 1(b)], of which the underlying physics will be discussed shortly. The maximum polariton interaction for various materials is calculated for the H1-cavity—QD system [see Supplementary Materials for details]. The results are listed in Table I, from which we find that MoS_2 and $MoSe_2$ monolayer QDs are best candidates for strongly interacting photonic systems. Fig. 1(c) shows that negative detuning can enhance interaction and reduce the kinetic energy of polaritons, favoring simulation of strongly interacting systems. A full survey of α versus the QD radius r_X and the detuning Δ is presented in Fig. 1(e).

TABLE I. Optimal polariton interaction for different materials in H1 cavity at zero exciton-photon detuning.

Materials	MoS_2	$MoSe_2$	GaAs	InAs	GaN
Optimal U_{pl} (meV)	0.85	0.48	0.32	0.16	0.51

Crossover from polariton blockade to photon blockade.— In the literature two regimes are known for photon anti-bunching: the photon blockade regime[15–18] where $U_X \gg \hbar\Omega$ and the polariton blockade regime[14] where $U_X \ll \hbar\Omega$. The Hamiltonian for the exciton-photon system with two energy quanta in a single cavity is

$$\mathcal{H}_{2q} = \begin{pmatrix} 2\hbar\omega_c & \sqrt{2}\hbar\Omega & 0 \\ \sqrt{2}\hbar\Omega & \hbar(\omega_c+\omega_X) & \sqrt{2}\hbar\Omega \\ 0 & \sqrt{2}\hbar\Omega & 2\hbar\omega_X + U_X \end{pmatrix}. \quad (5)$$

We plot the energy spectrum of the above Hamiltonian in Fig. 2(a). At exciton-photon resonance we can set the energy zero at $\hbar\omega_c = \hbar\omega_X$. The crossover is caused by the competition between the light-matter interaction $\hbar\Omega$ and exciton-exciton repulsion U_X.

The crossover between the two regimes is analyzed using the single- and two-photon correlation functions, $g^{(1)}(0)$ and $g^{(2)}(0)$, of the ground state of the Hamiltonian Eq. (5). Fig. 2(b) shows that with increasing exciton-exciton repulsion, the $g^{(2)}(0)$ correlation function is reduced. The $g^{(1)}(0)$ photon correlation function (representing the average photon number) considerably increases with prompted exciton-exciton repulsion.

To show the crossover from another aspect, we plot the two ratios U_{pl}/U_X and $U_{pl}/(\hbar\Omega)$ as functions of the dimensionless parameter $U_X/(\hbar\Omega)$ in Fig. 2(c). The dependences clearly indicate that in the polariton blockade regime ($U_X < \hbar\Omega$) the repulsive interaction U_{pl} is mainly determined by the exciton-exciton interaction U_X, while in the photon blockade regime ($U_X > \hbar\Omega$) the polariton interaction U_{pl} is rather limited by the exciton-photon interaction $\hbar\Omega$.

We now determine the phase diagram of the 1D interacting polariton system at zero exciton-photon detuning in Fig. 2(d). The polariton Mott insulator phase exists in the region with simultaneous strong exciton-exciton interaction and strong exciton-photon interaction. In other regions the system is in the polariton BEC phase. The Mott insulator phase has two regimes, the polariton blockade regime and the photon blockade regime, separated by the line $U_X = \hbar\Omega$. We remark that the statistics of photon, which can be characterized by the $g^{(1)}(0)$, $g^{(2)}(0)$ and higher-order photon correlation functions, are not uniquely determined by the phase or crossover boundaries. It is rather determined by the ground state wavefunction of the polariton[39].

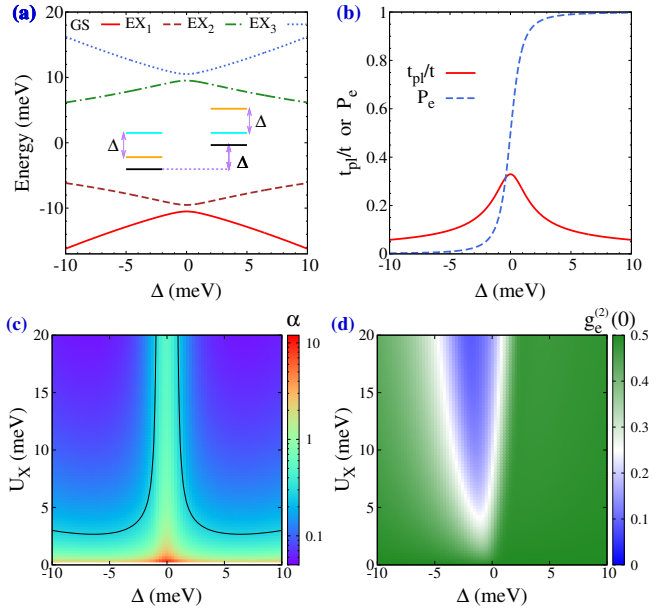

FIG. 3. Quantum simulation in 1D Cavity-QD superlattices. (a) Single-particle energy spectrum of coupled double cavity. Inset: Left (right) is the exciton (cyan), cavity (orange), lower polariton (black) energy levels for the even (odd) sites. The detuning at the even sites is positive, while at the odd sites it is negative. The energy difference between lower polariton levels in the two different sites is just the detuning Δ. (b) Hopping energy t_{pl}/t and the probability at even site P_e as functions of the detuning. (c) α and phase diagram (d) the photon correlation function at a even lattice site $g_e^{(2)}(0)$ versus U_X and Δ. Parameters for all figures: $t = 1$ meV and $\hbar\Omega = 10$ meV.

Superlattice of cavity-QD hybrid systems.— The above discussions are analogous to Mott transition of strongly interacting ultracold atoms in optical lattices[2, 3]. We now introduce the scheme in analog to optical *superlattices* which is realized using position-dependent detuning. For example, the detuning at even lattice sites is Δ, while for odd sites the detuning is $-\Delta$ [see the inset of Fig. 3(a)]. The single particle spectrum of a pair of such detuned cavities is plotted in Fig. 3(a). The splitting between the ground state and the first excited state is $\sqrt{\Delta^2 + t^2}$. Thus at large detuning $|\Delta|$ the full Hamiltonian can be truncated into the Hilbert space of the lowest energy state. For half-filling $\nu = 1/2$, the polaritonic Mott insulator phase is realized in the regime with $\Delta, \hbar\Omega, U_X \gg t$ [Figs. 3(b) and 3(c)]. For large positive Δ, the lowest energy state is mostly localized in the even sites, while the hopping energy between adjacent unit cells (a pair of even-odd sites) is suppressed [Fig. 3(b)]. We determine the phase boundary by $\alpha \equiv t_{pl}/U_{pl} = \alpha_c$ where U_{pl} is calculated in the same way as for the single cavity case [see Supplementary Materials]. The second-order correlation function for the photons emitted from the even site, $g_e^{(2)}(0)$, has a dip in the negative Δ region [Fig. 3(d)]. The photon anti-bunching is enhanced with increasing exciton repulsion U_X. For large negative detuning, the occupation at the even site is depleted as the even site has much higher energy than the odd site. Photons emerging at the even site are caused by quantum tunneling, of which the statistics is dominated by the tunneling rather than the interaction effect.

Realistic considerations.— Current fabrication technology can control the growth of photonic crystal cavity precisely, yielding very high quality factor[40]. High quality MoS_2 QDs with radius about 20 nm (suitable for strong polariton interaction) have been fabricated recently[23]. Very low temperature, about 100 mK, is needed to study the quantum phase transition, which is available using, e.g., dilution refrigerators. If the fluctuation among different cavities, a common problem in cavity-QD systems, can be suppressed by high-quality fabrication, the quantum simulation can be performed within current technology. Nevertheless, even a few coupled cavities[27] can provide a platform for quantum simulation of strongly interacting few-particle systems and serve as multi-photon entanglement light sources[42].

Acknowledgements.— J.H.J acknowledges supports from the faculty start-up funding of Soochow University. He also thanks Sajeev John, Gang Chen, Chao-Yang Lu, and Ming-Qi Weng for helpful discussions. H.X.W, Y.D.X and H.Y.C thank supports from the National Science Foundation of China for Excellent Young Scientists (no. 61322504). A.Z and A.M are supported by the National Science Foundation under grant NSF-EFRI-1433496; and the Air Force Office of Scientific Research-Young Investigator Program under grant FA9550-15-1-0150. A.M. also acknowledges useful discussions with Xiaodong Xu.

* joejhjiang@sina.com
† arka@uw.edu

[1] R. P. Feynman, Int. J. Theor. Phys. **21**, 467 (1982).
[2] M. Greiner, O.Mandel, T. Esslinger, T. W. Hansch, and I. Bloch, Nature (London) **415**, 39 (2002).
[3] I. Bloch, J. Dalibard, and S. Nascimbene, Nature Phys. **8**, 267 (2012).
[4] D. E. Chang, V.Vuletić, and M. D. Lukin, Nat. Photon. **8**, 685 (2014).
[5] S. Buckley, K. Rivoire, and J.Vučković, Rep. Prog. Phys. **75**, 126503 (2012).
[6] I. Carusotto and C. Ciuti, Rev. Mod. Phys. **85**, 299 (2013).
[7] T. Byrnes, N. Y. Kim, and Y. Yamamoto, Nature Phys. **10**, 803 (2014).
[8] J.-H. Jiang and S. John, Phys. Rev. X **4**, 031025 (2014).
[9] J. Kasprzak et al., Nature (London) **443**, 409 (2006).
[10] R. Balili, V. Hartwell, D. Snoke, L. Pfeiffer, and K. West, Science **316**, 1007 (2007).

[11] J. H. Jiang and S. John, Sci. Rep. **4**, 7432 (2014).
[12] H. S. Nguyen et al., Phys. Rev. Lett. **110**, 236601 (2013).
[13] D.Ballarini et al., Nat. Commun. **4**, 1778 (2013).
[14] A. Verger, C. Ciuti, and I. Carusotto, Phys. Rev. B **73**, 193306 (2006).
[15] K. M. Birnbaum, A. Boca, R. Miller, A. D. Boozer, T. E. Northup, and H. J. Kimble, Nature (London) **436**, 87 (2005).
[16] A. Faraon, I. Fushman, D. Englund, N. Stoltz, P. Petroff, and J. Vučković, Nature Phys. **4**, 859 (2008).
[17] A. Reinhard, T. Volz, M. Winger, A. Badolato, K. J. Hennessy, E. L. Hu, and A. Imamoğlu, Nat. Photon. **6**, 93 (2012).
[18] K. Müller et al., Phys. Rev. Lett. **114**, 233601 (2015).
[19] J.Hagemeier et al., Opt. Exp. **20**, 24714 (2012).
[20] K. F. Mak, C. Lee, J. Hone, J. Shan, and T. F. Heinz, Phys. Rev. Lett. **105**, 136805 (2010).
[21] Q. H. Wang, K. Kalantar-Zadeh, A. Kis, J. N. Coleman, and M. S. Strano, Nat. Nanotech. **7**, 699 (2012).
[22] X. Xu, W. Yao, D. Xiao, and T. F. Heinz, Nature Phys. **10**, 343 (2014).
[23] G.Wei et al., arXiv: 1510.09135.
[24] M. M. Ugeda et al., Nat. Mater. **13**, 1091 (2014).
[25] X. Liu, T. Galfsky, Z. Sun, F. Xia, E.-c. Lin, Y.-H. Lee, S. Kéna-Cohen, and V. M. Menon, Nat. Photon. **9**, 30 (2015).
[26] S.Dufferwiel et al., Nat. Commun. **6**, 8579 (2015).
[27] S.Wu et al., Nature (London) **520**, 69 (2015).
[28] Y.Ye et al., Nat. Photon. **9**, 733 (2015).
[29] O. Salehzadeh, M. Djavid, N. H. Tran, I. Shih, and Z. Mi, Nano Lett. **15**, 5302 (2015).
[30] Y.-M. He et al., Nat. Nanotech. **10**, 497 (2015).
[31] A. Srivastava et al., Nat. Nanotech. **10**, 491 (2015).
[32] M. Koperski et al., Nat. Nanotech. **10**, 503 (2015).
[33] C. Chakraborty, L. Kinnischtzke, K. M. Goodfellow, R.Beams, and A. N. Vamivakas, Nat. Nanotech. **10**, 507 (2015).
[34] D. Y. Qiu, F. H. da Jornada, and S. G. Louie, Phys. Rev. Lett. **111**, 216805 (2013).
[35] F.Tassone and Y.Yamamoto, Phys. Rev. B **59**, 10830 (1999).
[36] H. Shi et al., ACS nano. **7**, 1072 (2013).
[37] A. Majumdar, A. Rundquist, M. Bajcsy, V. D. Dasika, S. R. Bank, and J.Vučković, Phys. Rev. B **86**, 195312 (2012).
[38] T. D. Kühner and H.Monien, Phys. Rev. B **58**, R14741 (1998).
[39] S. Yang and S. John, Phys. Rev. B **84**, 024515 (2011).
[40] S. Noda, M. Fujita, and T. Asano, Nat. Photon. **1**, 449 (2007).
[41] Z. Jin, X. Li, J. T. Mullen, and K. W. Kim, Phys. Rev. B **90**, 045422 (2014).
[42] J.-W. Pan, Z.-B. Chen, C.-Y. Lu, H. Weinfurter, A. Zeilinger, and M. Zukowski, Rev. Mod. Phys. **84**, 777 (2012).